Letter to the Editor

Noninvasive multimodality imaging in hereditary transthyretin amyloid cardiomyopathy: a family case series from the southeast coast of China with an identified heterozygous missense mutation c.349G>T in the transthyretin gene

Qianni Du^, Hengyu Zhao

Department of Radiology, Xiamen Cardiovascular Hospital of Xiamen University, School of Medicine, Xiamen University, Xiamen, China

Correspondence to: Qianni Du, MM. Department of Radiology, Xiamen Cardiovascular Hospital of Xiamen University, School of Medicine, Xiamen University, No. 2999 Jinshan Road, Huli District, Xiamen 361000, China. Email: 1319532367@qq.com.

Submitted Jan 08, 2023. Accepted for publication Jun 09, 2023. Published online Jun 29, 2023.
doi: 10.21037/qims-23-39
View this article at: https://dx.doi.org/10.21037/qims-23-39

Introduction

Transthyretin amyloid cardiomyopathy (ATTR-CM) is a manifestation of cardiac involvement in systemic amyloidosis. Transthyretin deposits in the heart after misfolding into amyloid fibrils, resulting in restrictive cardiomyopathy with heart failure and arrhythmias. According to the transthyretin gene (*TTR*) mutation, ATTR-CM is divided into hereditary transthyretin amyloid cardiomyopathy (hATTR-CM) and wild-type transthyretin amyloid cardiomyopathy (wtATTR-CM) (1,2). Although endomyocardial biopsy (EMB) is the "gold standard" for ATTR-CM diagnosis, it is an invasive operation, which reduces patient acceptance (3). At the same time, the distribution of amyloid deposition is uneven, and the randomness and blindness of sampling can also lead to low diagnostic sensitivity. Increasing evidence from epidemiological studies has suggested that ATTR-CM is not as rare as previously proposed (4-6). In the past, the main reason for the low diagnostic rate of ATTR-CM was the lack of noninvasive screening methods with high sensitivity and specificity. Recent advances in noninvasive imaging techniques, such as echocardiography, cardiac magnetic resonance (CMR) imaging, and nuclear cardiac imaging, have made it possible to diagnose ATTR-CM easily and accurately (3,7). In this paper, we report the diagnostic procedures of 2 siblings who presented with transthyretin amyloidosis cardiomyopathy diagnosed by multimodality imaging.

Case presentation

Case 1

A 64-year-old woman presented with a 3-year history of shortness of breath after activity, occasionally accompanied by nocturnal asthma, and in the last week, symptoms such as nausea, vomiting, loss of appetite, and the addition of some urinary incontinence had occurred intermittently. Her N-terminal pro-B-type natriuretic peptide (NT-proBNP) level was significantly elevated, and high-sensitivity cardiac troponin T (hs-cTnT) was in the normal levels.

Conventional transthoracic echocardiography was performed, which showed left ventricular (LV) and right ventricular (RV) hypertrophy with a granular sparkling appearance of the interventricular septum. The other abnormal echocardiographic findings included small ventricular cavity size; interatrial septal thickening with the granular sparkling pattern; thickened valves; biatrial enlargement; and pericardial effusion (*Figure 1A*). To

^ ORCID: 0000-0002-4134-0285.

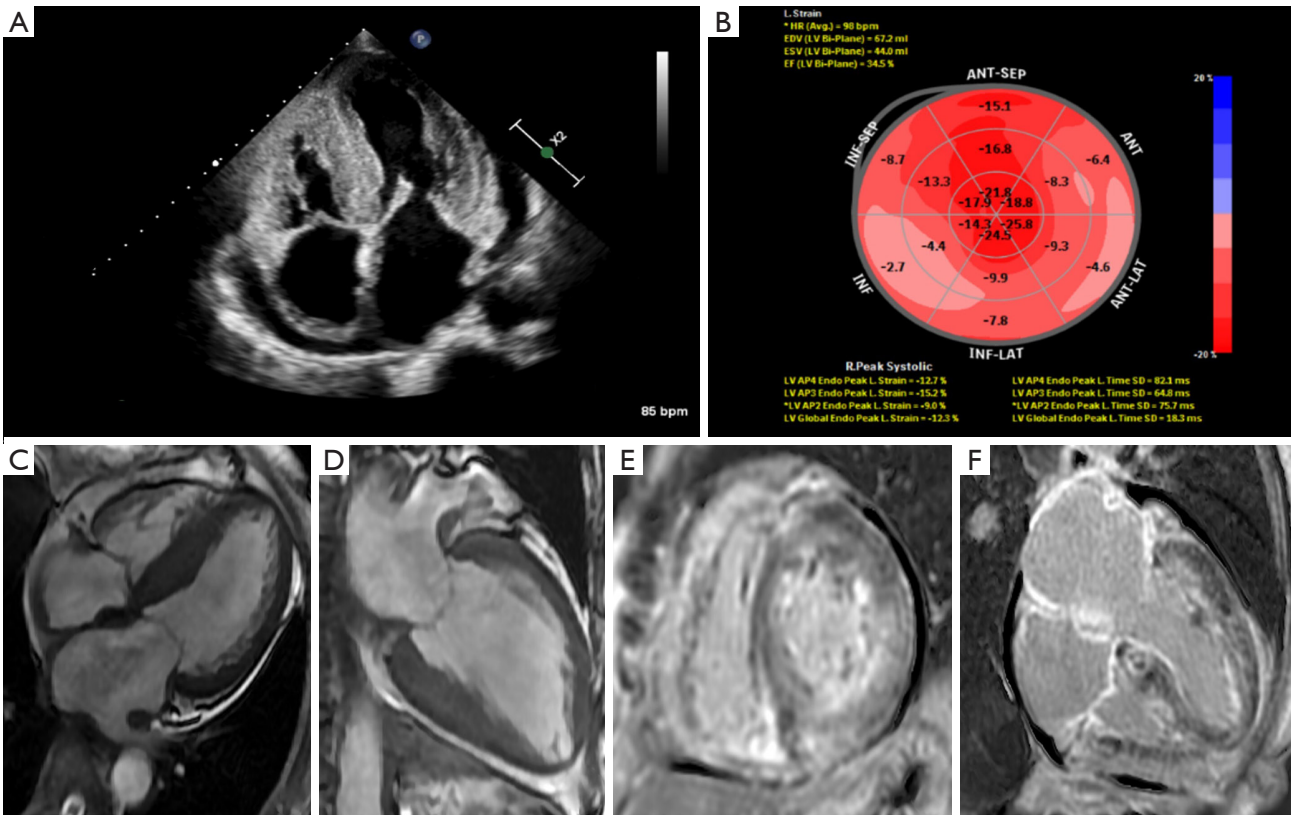

Figure 1 Echocardiography and CMR findings in Case 1. (A) Apical 4-chamber view of echocardiography demonstrates LV and RV hypertrophy with a granular sparkling appearance of the interventricular septum; small ventricular cavity size, interatrial septal thickening with the granular sparkling pattern, thickened valves, biatrial enlargement, and pericardial effusion. (B) Bullseye map of speckle tracking echocardiography demonstrates LV global longitudinal strain decreased; reduced longitudinal contractility was mainly noted at the basal segments (red denotes normal longitudinal strain and pink denotes abnormal longitudinal strain); EF was 34.5%. (C,D) 4- and 2-chamber view cines of CMR show asymmetric LV hypertrophy with the most severe hypertrophy involving the interventricular septum. Note the thickened interatrial septum in the 4-chamber view cine imaging. (E,F) Short-axis and 4-chamber view of phase-sensitive inversion recovery late gadolinium enhancement show LV and RV wall diffuse subendocardial hyper-enhancement. Along with subendocardial LGE in the ventricle, LGE may also be seen in the atrial wall, interatrial septum, and atrioventricular valves. HR, heart rate; Avg., average; EDV, end-diastolic volume; LV, left ventricular; ESV, end-systolic volume; EF, ejection fraction; ANT, anterior; SEP, septal; INF, inferior; LAT, lateral; SD, standard deviation; CMR, cardiac magnetic resonance; RV, right ventricular; LGE, late gadolinium enhancement.

further examine LV myocardial performance, 2-dimensional (2D) speckle tracking echocardiography-derived (STE-derived) measurement of LV strain and strain rate was performed, which showed that the LV global longitudinal strain was decreased. Reduced longitudinal contractility was mainly noted at the basal segments. The LV ejection fraction (EF) was 34.5% (*Figure 1B*). A CMR was also performed, which showed asymmetric LV hypertrophy and a diffuse pattern of late gadolinium enhancement (LGE) at inversion recovery sequences (*Figure 1C-1F*), suggesting cardiac amyloidosis. Echocardiography and CMR showed thickening of the ventricular wall, whereas the electrocardiogram (ECG) showed reversed R-wave progression in V1–V5 (*Figure 2*), which was also suggestive of cardiac amyloidosis. Based on these findings, a diagnosis of cardiac amyloidosis was considered. However, we were unable to definitively distinguish ATTR from light-chain (AL) cardiac amyloidosis.

Therefore, serum-free light chain assay and serum and urine protein electrophoresis with immunofixation were performed, the results of which were negative. Hence, the patient underwent ^{99m}Technetium-pyrophosphate (^{99m}Tc-

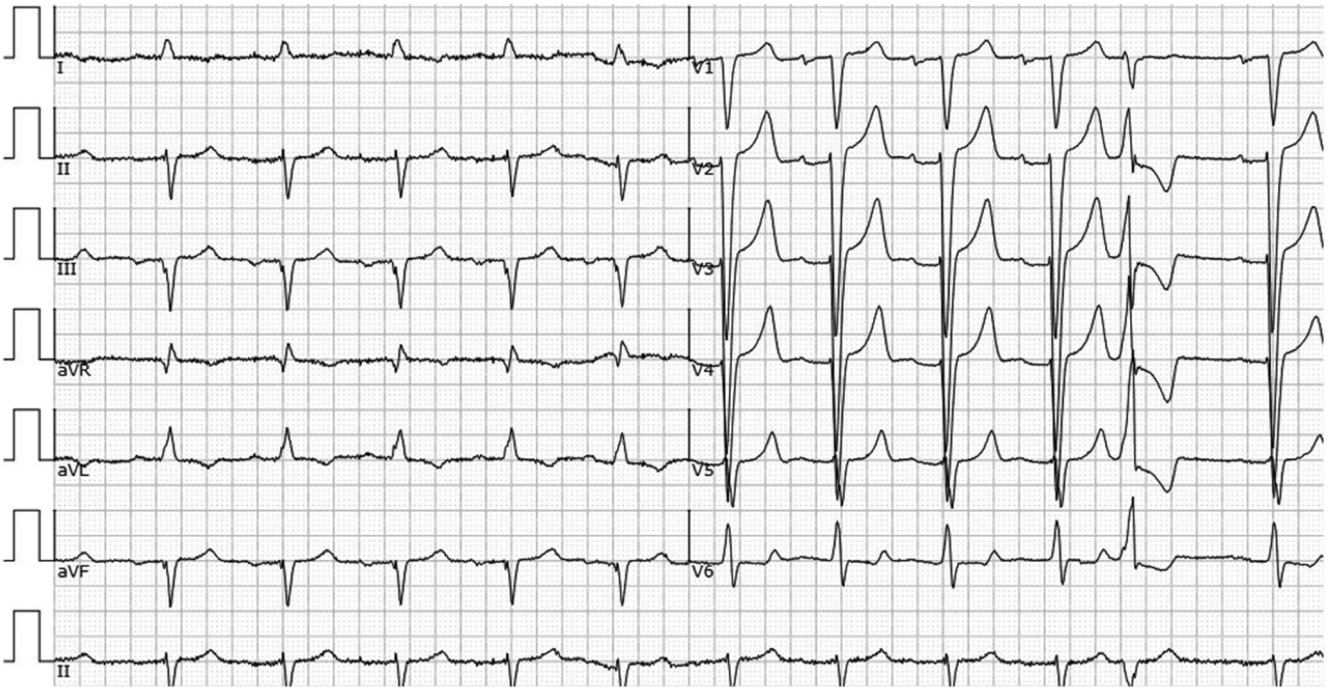

Figure 2 Electrocardiogram on admission from Case 1. Electrocardiogram shows first-degree atrioventricular block; non-specific intraventricular block; ventricular premature beat; and reversed R-wave progression in V1–V5. aVR, augmented vector right; aVL, augmented vector left; aVF, augmented vector foot.

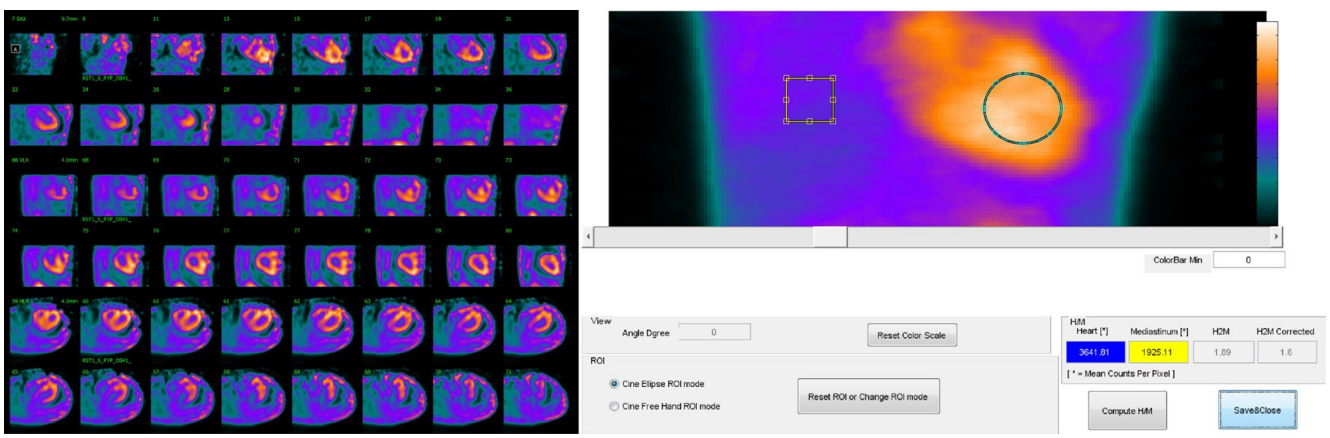

Figure 3 ^{99m}Tc-PYP scintigraphy findings in Case 1. ^{99m}Tc-PYP SPECT scan with Grade 3 ^{99m}Tc-PYP uptake. On the right is the corresponding H/CL 1.89. ROI, region of interest; ^{99m}Tc-PYP, ^{99m}Technetium-pyrophosphate; SPECT, single-photon emission computerized tomography; H/CL, heart-to-contralateral lung ratio.

PYP) scintigraphy. The visual semi-quantitative score (Perugini scoring system) was 3, and the quantitative heart-to-contralateral lung ratio (H/CL) was 1.89 (*Figure 3*). Therefore, a diagnosis of ATTR-CM was feasible.

Finally, deoxyribonucleic acid (DNA) sequencing of the *TTR* gene revealed a proven heterozygous missense mutation c.349G>T in exon 4 of *TTR*, resulting in the replacement of alanine with serine at position 117 of the

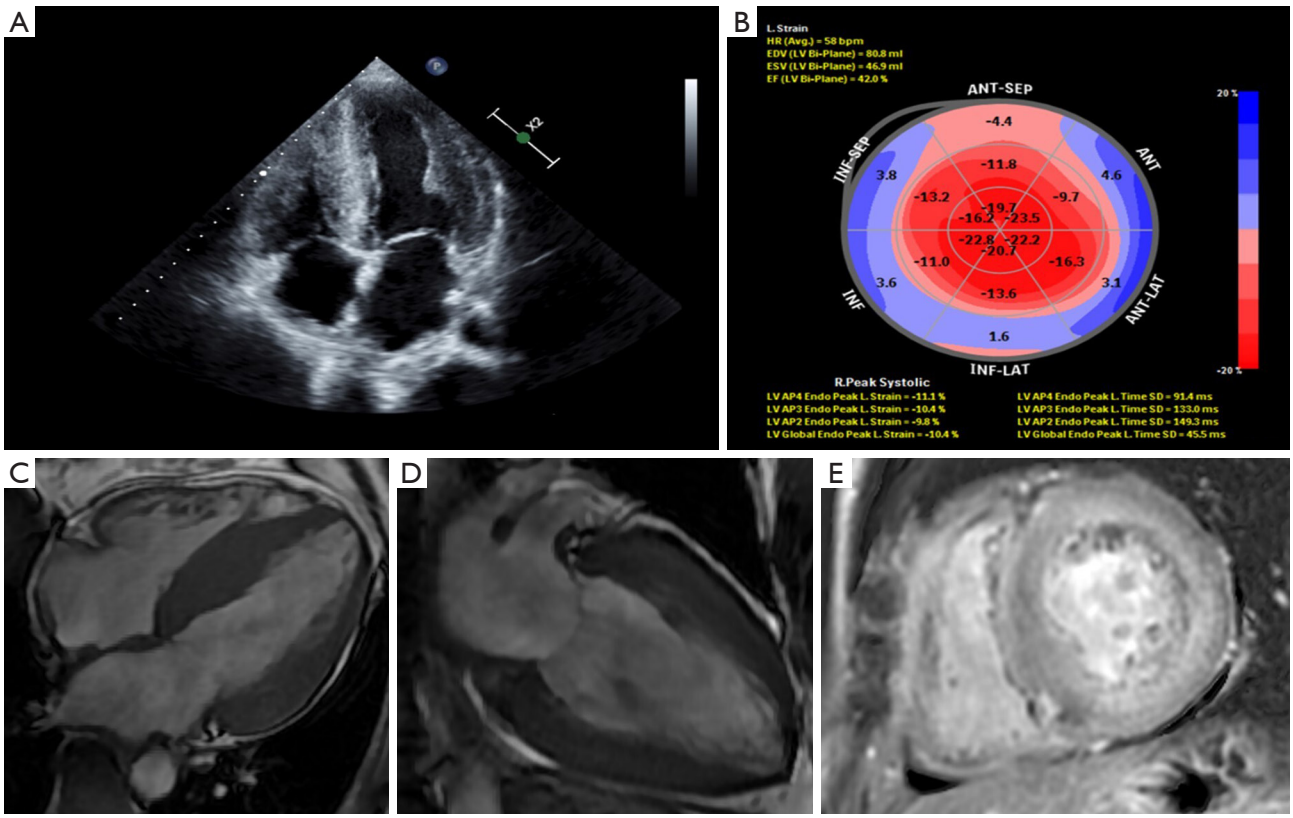

Figure 4 Echocardiography and CMR findings in Case 2. (A) Apical 4-chamber view of echocardiography shows LV and RV hypertrophy with a granular sparkling appearance of the interventricular septum; interatrial septal thickening with the granular sparkling pattern; and biatrial enlargement. (B) Bullseye map of speckle tracking echocardiography demonstrates LV global longitudinal strain decreased with the "cherry-on-the-top" sign (red denotes normal longitudinal strain at the apex and pink/blue denotes abnormal longitudinal strain at the mid/basal left ventricle); EF was 42.0%. (C,D) 4- and 2-chamber view cines of CMR show significant concentric LV hypertrophy. The thickened interatrial septum is also noted in the 4-chamber view cine imaging. (E) Short-axis view of phase-sensitive inversion recovery LGE shows global subendocardial circumferential enhancement of left ventricular wall. HR, heart rate; Avg., average; EDV, end-diastolic volume; LV, left ventricular; ESV, end-systolic volume; EF, ejection fraction; ANT, anterior; SEP, septal; INF, inferior; LAT, lateral; SD, standard deviation; CMR, cardiac magnetic resonance; RV, right ventricular; LGE, late gadolinium enhancement.

mature protein (Ala117Ser). Thus, the diagnosis of hATTR-CM was confirmed.

Case 2

Some 18 months later, a 59-year-old man (the younger brother of Case 1) carried out a routine physical examination after presenting with a 1-week history of abdominal bloating, which revealed an abnormal ECG. The NT-proBNP level was significantly elevated, and hs-cTnT levels were in the normal range.

The typical echocardiographic and CMR findings were strongly suggestive of cardiac amyloidosis (*Figure 4*). Perugini grade 3 and an H/CL ratio of 2.47 on ^{99m}Tc-PYP scan suggested ATTR subtype amyloidosis (*Figure 5*).

However, the result of urine protein electrophoresis with immunofixation was abnormal. Finally, the diagnosis was confirmed by immunoelectron microscopy, showing Kappa (–), Lambda (–), and TTR (+++).

Genetic testing revealed that his mutation site was consistent with that of his older sister.

All procedures performed in this study were in accordance with the ethical standards of the institutional and/or national research committee(s) and with the Helsinki Declaration (as revised in 2013). Written informed consent was provided by the patients for publication of this case

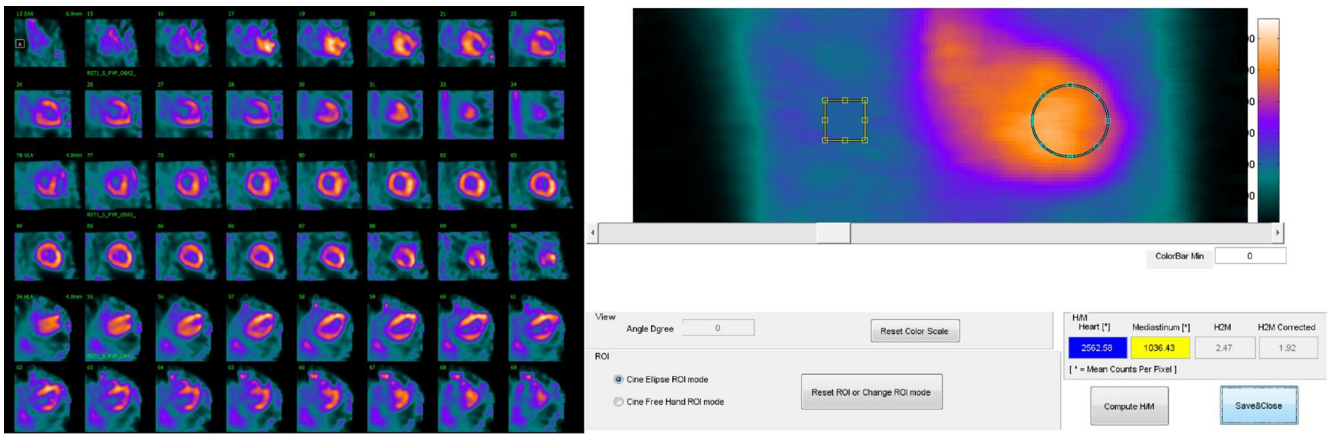

Figure 5 ^{99m}Tc-PYP scintigraphy findings in Case 2. ^{99m}Tc-PYP SPECT scan with Grade 3 ^{99m}Tc-PYP uptake. On the right is the corresponding H/CL 2.47. ROI, region of interest; ^{99m}Tc-PYP, ^{99m}Technetium-pyrophosphate; SPECT, single-photon emission computerized tomography; H/CL, heart-to-contralateral lung ratio.

report and accompanying images. A copy of the written consent is available for review by the editorial office of this journal.

Discussion

hATTR-CM is a severe, heterogeneous multisystem condition caused by mutations of *TTR*. More than 150 different *TTR* mutations have been reported to date, with different mutations causing discrete disease manifestations. The mutation c.349G>T was found in 2 siblings in this case series. The *TTR* mutation c.349G>T has mainly been reported in southern China, including Taiwan (8-11). Although researchers in both Malaysia and Singapore have reported the c.349G>T mutation, the specific patients had previously migrated from southern China (12,13). The prevalence of various mutations varies by race and location. The most common mutation found in the above studies is Ala117Ser. This is not the case in northern China, where the most common mutations are Gly47Arg and Val30Met (9,14). The phenotypic and genotypic spectra of hATTR differ significantly. The majority of reported *TTR* Ala117Ser mutation patients have initially presented with neurological dysfunction (8,10,11). In this study, Case 1 had nocturnal asthma, nausea, vomiting, loss of appetite, and urinary incontinence, whereas Case 2 had abdominal bloating, indicating neurological involvement. Initially, Case 1 consulted a gastroenterologist, who had not made the connection between ATTR and the patient's chief complaint. The patient was later referred to our hospital because of heart failure. Using noninvasive multimodality imaging, she was diagnosed with the ATTR subtype. This case series verifies that multimodality imaging plays an important role in the diagnosis of cardiac amyloidosis, especially for the ATTR subtype.

Cardiac involvement frequently indicates the clinical course of the disease (8,12). Case 2 had no cardiac complaints, but several supplementary examinations revealed abnormalities. For high-risk populations, especially gene-positive patients with a family history, early screening is extremely important. Therefore, it is important to discuss the best screening strategy for cardiac amyloidosis in gene-positive populations at an earlier stage. Although serum biomarkers and electrocardiograms are frequently used to evaluate the risk of cardiac amyloidosis, neither of these tests can be used to diagnose amyloidosis on their own. As a result, early detection with imaging remains a crucial component of the diagnostic process for cardiac amyloidosis. The evaluation of cardiac amyloidosis using echocardiography focuses on morphological findings related to amyloid infiltration. CMR can detect early cardiac involvement and offer morphological structure, functional evaluation, and tissue characteristics. Several studies have demonstrated the high sensitivity and specificity of ^{99m}Tc-PYP scanning in the diagnosis of ATTR-CM, which may aid in its early detection (3,15-20). Although multiple imaging examinations can detect cardiac involvement in amyloidosis, the appropriate utilization ratings for echocardiography, CMR, and ^{99m}Tc-PYP for *TTR* carriers in the initial evaluation and recurrent testing remain

uncertain. The patients in this case series had complete imaging data, and the patient in Case 2 was detected as aberrant prior to the onset of cardiac symptoms. The H/CL ratio on the ^{99m}Tc-PYP scan appears to be connected to the LGE of CMR. There remains a need to validate the best screening strategy for *TTR* gene carriers and to expand the genetic testing population in the pedigree analysis with known familial amyloidosis. Prospective studies evaluating the diagnostic value of noninvasive imaging techniques, including echocardiography, ^{99m}Tc-PYP, and CMR should be undertaken in *TTR* carriers. The patient in Case 2 was diagnosed at an earlier stage and treated promptly, perhaps improving their prognosis.

The missense variant c.349G>T (p.Ala117Ser) of *TTR* may be responsible for the occurrence of ATTR in the family from southern China. *TTR* gene testing provides a cost-effective approach to identify high-risk populations. Early detection with imaging and early diagnosis of hATTR-CM should be followed by timely and appropriate therapy to improve the prognosis of patients. The research findings from the hATTR subgroup can be applied to a larger group of ATTR patients.

Acknowledgments

Funding: None.

Footnote

Conflicts of Interest: Both authors have completed the ICMJE uniform disclosure form (available at https://qims.amegroups.com/article/view/10.21037/qims-23-39/coif). The authors have no conflicts of interest to declare.

Ethical Statement: The authors are accountable for all aspects of the work in ensuring that questions related to the accuracy or integrity of any part of the work are appropriately investigated and resolved. All procedures performed in this study were in accordance with the ethical standards of the institutional and/or national research committee(s) and with the Helsinki Declaration (as revised in 2013). Written informed consent was provided by the patients for publication of this case report and accompanying images. A copy of the written consent is available for review by the editorial office of this journal.

References

1. Garcia-Pavia P, Rapezzi C, Adler Y, Arad M, Basso C, Brucato A, et al. Diagnosis and treatment of cardiac amyloidosis: a position statement of the ESC Working Group on Myocardial and Pericardial Diseases. Eur Heart J 2021;42:1554-68.
2. Kittleson MM, Maurer MS, Ambardekar AV, Bullock-Palmer RP, Chang PP, Eisen HJ, Nair AP, Nativi-Nicolau J, Ruberg FL; American Heart Association Heart Failure and Transplantation Committee of the Council on Clinical Cardiology. Cardiac Amyloidosis: Evolving Diagnosis and Management: A Scientific Statement From the American Heart Association. Circulation 2020;142:e7-e22.
3. Dorbala S, Ando Y, Bokhari S, Dispenzieri A, Falk RH, Ferrari VA, et al. ASNC/AHA/ASE/EANM/HFSA/ISA/SCMR/SNMMI Expert Consensus Recommendations for Multimodality Imaging in Cardiac Amyloidosis: Part 1 of 2-Evidence Base and Standardized Methods of Imaging. Circ Cardiovasc Imaging 2021;14:e000029.
4. González-López E, Gallego-Delgado M, Guzzo-Merello G, de Haro-Del Moral FJ, Cobo-Marcos M, Robles C, Bornstein B, Salas C, Lara-Pezzi E, Alonso-Pulpon L, Garcia-Pavia P. Wild-type transthyretin amyloidosis as a cause of heart failure with preserved ejection fraction. Eur Heart J 2015;36:2585-94.
5. Hahn VS, Yanek LR, Vaishnav J, Ying W, Vaidya D, Lee YZJ, et al. Endomyocardial biopsy characterization of heart failure with preserved ejection fraction and prevalence of cardiac amyloidosis. JACC Heart Fail 2020;8:712-24.
6. Lund LH, Eldhagen P. Diagnosing heart failure with preserved ejection fraction in cardiac amyloidosis or diagnosing cardiac amyloidosis in heart failure with preserved ejection fraction? Eur J Heart Fail 2022;24:2387-9.
7. Dorbala S, Ando Y, Bokhari S, Dispenzieri A, Falk RH, Ferrari VA, et al. ASNC/AHA/ASE/EANM/HFSA/ISA/SCMR/SNMMI Expert Consensus Recommendations for Multimodality Imaging in Cardiac Amyloidosis: Part 2 of 2-Diagnostic Criteria and Appropriate Utilization. Circ

Cardiovasc Imaging 2021;14:e000030.
8. Wang S, Peng W, Pang M, Mao L, Peng D, Yu B, Wu S, Hu D, Yang Y, He J, Ouyang M. Clinical Profile and Prognosis of Hereditary Transthyretin Amyloid Cardiomyopathy: A Single-Center Study in South China. Front Cardiovasc Med 2022;9:900313.
9. Du K, Li F, Wang H, Miao Y, Lv H, Zhang W, Wang Z, Yuan Y, Meng L. Hereditary transthyretin amyloidosis in mainland China: a unicentric retrospective study. Ann Clin Transl Neurol 2021;8:831-41.
10. Hsu HC, Liao MF, Hsu JL, Lo AL, Kuo HC, Lyu RK, Wu VC, Wang CW, Ro LS. Phenotypic expressions of hereditary Transthyretin Ala97Ser related Amyloidosis (ATTR) in Taiwanese. BMC Neurol 2017;17:178.
11. Lin YH, Hsueh HW, Su MY, Cheng MF, Chiang MC, Juang JJ, Kao YH, Chang KC, Feng FP, Hsieh ST, Chao CC. Cardiomyopathy correlates to nerve damage in p.A117S late-onset transthyretin amyloid polyneuropathy. Ann Clin Transl Neurol 2022;9:1359-69.
12. Chen Z, Koh JS, Saini M, Tay KSS, Jayne Tan Y, Chai JYH, Fam SR, Juraidah AR, Lim PK, Ng ASL, Prasad K, Tan CB, Umapathi T, Verma KK, Yong MH, Yu C, Ng PS. Hereditary Transthyretin Amyloidosis- Clinical and Genetic Characteristics of a Multiracial South-East Asian Cohort in Singapore. J Neuromuscul Dis 2021;8:723-33.
13. Goh KJ, Hun J, Joon B, Tan CT. Familial transthyretin-related amyloid polyneuropathy in a Malaysian patient of ethnic Chinese descent [Internet]. 2008 [cited 2023 May 3]. Available online: https://www.researchgate.net/publication/266094054_Familial_transthyretin-related_amyloid_polyneuropathy_in_a_Malaysian_patient_of_ethnic_Chinese_descent
14. He S, Tian Z, Guan H, Li J, Fang Q, Zhang S. Clinical characteristics and prognosis of Chinese patients with hereditary transthyretin amyloid cardiomyopathy. Orphanet J Rare Dis 2019;14:251.
15. Dorbala S, Cuddy S, Falk RH. How to Image Cardiac Amyloidosis: A Practical Approach. JACC Cardiovasc Imaging 2020;13:1368-83.
16. Maurer MS, Bokhari S, Damy T, Dorbala S, Drachman BM, Fontana M, Grogan M, Kristen AV, Lousada I, Nativi-Nicolau J, Cristina Quarta C, Rapezzi C, Ruberg FL, Witteles R, Merlini G. Expert Consensus Recommendations for the Suspicion and Diagnosis of Transthyretin Cardiac Amyloidosis. Circ Heart Fail 2019;12:e006075.
17. Ruberg FL, Grogan M, Hanna M, Kelly JW, Maurer MS. Transthyretin Amyloid Cardiomyopathy: JACC State-of-the-Art Review. J Am Coll Cardiol 2019;73:2872-91.
18. Tahara N, Lairez O, Endo J, Okada A, Ueda M, Ishii T, Kitano Y, Lee HE, Russo E, Kubo T. (99m) Technetium-pyrophosphate scintigraphy: a practical guide for early diagnosis of transthyretin amyloid cardiomyopathy. ESC Heart Fail 2022;9:251-62.
19. Witteles RM, Bokhari S, Damy T, Elliott PM, Falk RH, Fine NM, Gospodinova M, Obici L, Rapezzi C, Garcia-Pavia P. Screening for Transthyretin Amyloid Cardiomyopathy in Everyday Practice. JACC Heart Fail 2019;7:709-16.
20. Ioannou A, Patel RK, Razvi Y, Porcari A, Sinagra G, Venneri L, et al. Impact of Earlier Diagnosis in Cardiac ATTR Amyloidosis Over the Course of 20 Years. Circulation 2022;146:1657-70.

Cite this article as: Du Q, Zhao H. Noninvasive multimodality imaging in hereditary transthyretin amyloid cardiomyopathy: a family case series from the southeast coast of China with an identified heterozygous missense mutation c.349G>T in the transthyretin gene. Quant Imaging Med Surg 2023;13(8):5436-5442. doi: 10.21037/qims-23-39

